Supporting Information

$Ni_2P_2O_7$ Nanoarrays with Decorated C_3N_4 Nanosheets as Efficient Electrode for Supercapacitors

Ning Zhang,[*, †] Chen Chen, [†] Yule Chen, [†] Gen Chen, [†] Chengan Liao, [†] Bo Liang, [†] Jisheng Zhang,[†] An Li,[†] Baopeng Yang,[†] Zhihe Zheng,[†] Xiaohe Liu,[*, †] Anqiang Pan,[†] Shuquan Liang,[†] and Renzhi Ma[*, ‡]

[†] School of Materials Science and Engineering, Central South University, Changsha, Hunan 410083, China

[‡] International Center for Materials Nanoarchitectonics (MANA), National Institute for Materials Science (NIMS), 1−1 Namiki, Tsukuba, Ibaraki 305−0044, Japan

*E−mail: nzhang@csu.edu.cn (N. Zhang);

liuxh@csu.edu.cn (X. Liu);

ma. renzhi@nims.go.jp (R. Ma).

Experimental Section

Materials Characterization

X−ray diffraction profiles were recorded by a RIGAKU Rint−2000 X−ray diffractometer equipped with graphite monochromatized Cu−Kα radiation (λ=1.54184 Å). Scanning electron microscopy and energy dispersive spectrometer mapping images was collected on a FEI Helios Nanolab 600i field emission scanning electron microscopy. Transmission electron microscopy images was produced from a FEI Tecnai G2 F20 field emission transmission electron microscopy operated at 200 kV. The X−ray photoelectron spectroscopy spectra were recorded from a Thermo Fisher ESCALAB 250Xi spectrophotometer. Fourier transform infrared spectrometer Thermo Fisher IS10 infrared spectrometer.

Three−electrodes electrochemical measurement: Electrochemical properties was measured on a Gamry Interface 1000 electrochemistry workstation in a three electrode cell by using the fabricated materials as working electrode without further treatment. Hg/HgO electrode was used as reference electrode, platinum plat electrode was acted as counter electrode, and 3 M KOH was applied as electrolyte. The cyclic voltammetry (CV), galvanostatic charge/discharge (GCD), and electrochemical impedance spectroscopy (EIS) were recorded. According to the galvanostatic discharge curves, the corresponding specific capacitance was evaluated by such an equation: C_{sc} = (I Δt) / (S ΔV), where the C_{sc} was the specific capacitance, I (A) was the discharge current, Δt (s) was the discharge time, S (cm^2) was the areas of active materials on Ni foam, and ΔV (V) was the volt window.[1]

Fabrication asymmetric supercapacitor cells

The asymmetric supercapacitor was assembled by utilizing Ni foam supported materials as positive electrode, active carbon as negative electrode, 3 M KOH as the electrolyte, and a diaphragm to separate the positive and negative electrodes. To obtain a best specific capacitance of ASCs, the charge balance the relationship between the two electrodes should

conform to $q^+ = q^-$. The mass of active materials between the two electrodes are adjusted as the following equations: $q = C \times \Delta V \times m$, $m^+/m^- = (C^- \times \Delta V^-) / (C^+ \times \Delta V^+)$, where m (g) was the active material mass on the electrode, C (F g^{-1}) was specific capacitance of electrode, and the ΔV (V) was the potential window.[2]

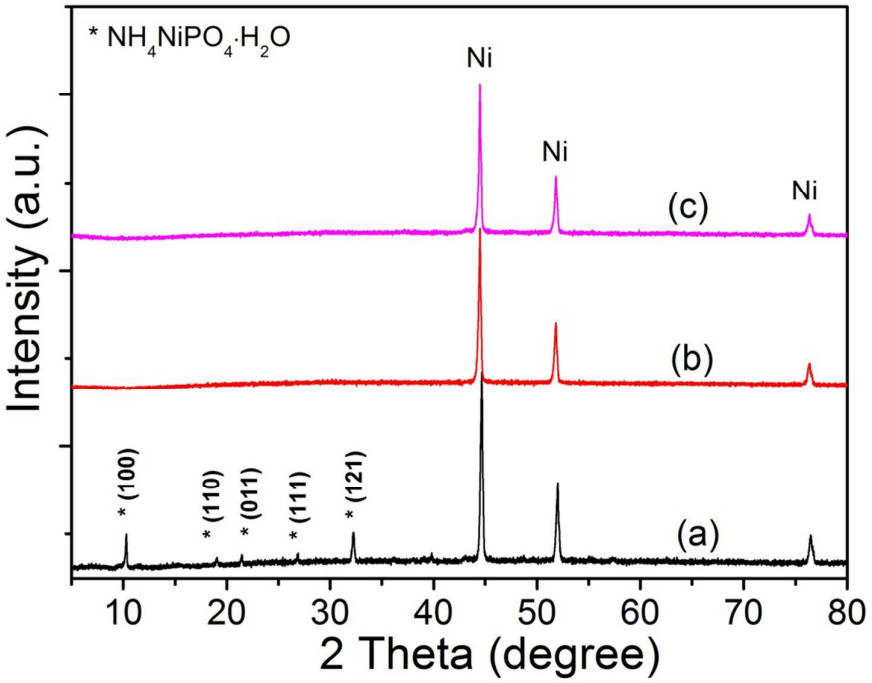

Figure S1 XRD profiles of (a) Ni foam supported $NH_4NiPO_4 \cdot H_2O$; (b) Ni foam/$Ni_2P_2O_7$, and (c) C_3N_4 coated Ni foam/$Ni_2P_2O_7$.

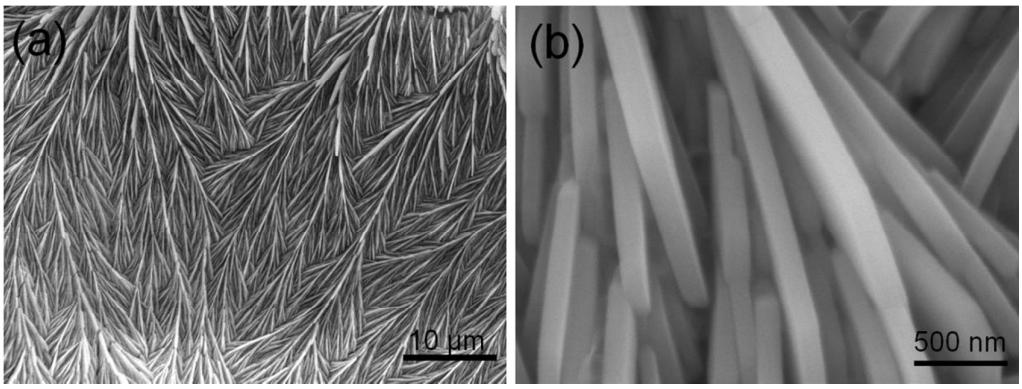

Figure S2 (a-b)SEM image of Ni foam supported $NH_4NiPO_4 \cdot H_2O$.

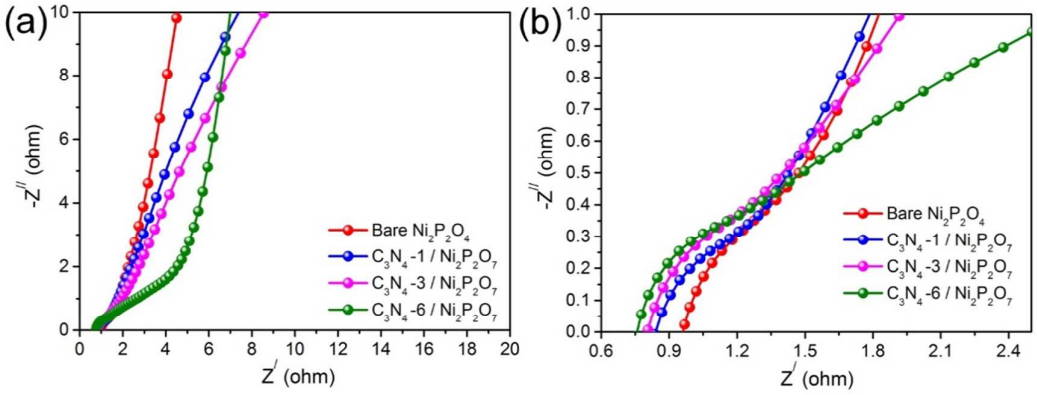

Figure S3 (a) EIS plots of the products; (b) enlarged curves at high frequency region.

The impedance electrochemical impedance spectroscopy was compared, as shown in Figure S3. The EIS data shows a solution resistance (Rs) and a charge–transfer resisitance (Rct). A vertical line leaning to imaginary axis represents the value of Rs. As can be seen from the inset, Rs value are 0.96, 0.85, 0.81, and 0.76 Ω for bare $Ni_2P_2O_7$, C_3N_4-1/$Ni_2P_2O_7$, C_3N_4-3/$Ni_2P_2O_7$, and C_3N_4-6/$Ni_2P_2O_7$, respectively. At high frequency region, it displays a negligible semicircle, revealing the low charge transfer resistence for Ni foam with pasted $Co_{0.2}Ni_{0.8}$ pyrophosphates. The Rct value are 0.87, 0.94, 1.03, and 1.08 Ω for bare $Ni_2P_2O_7$, C_3N_4-1/$Ni_2P_2O_7$, C_3N_4-3/$Ni_2P_2O_7$, and C_3N_4-6/$Ni_2P_2O_7$, respectively.

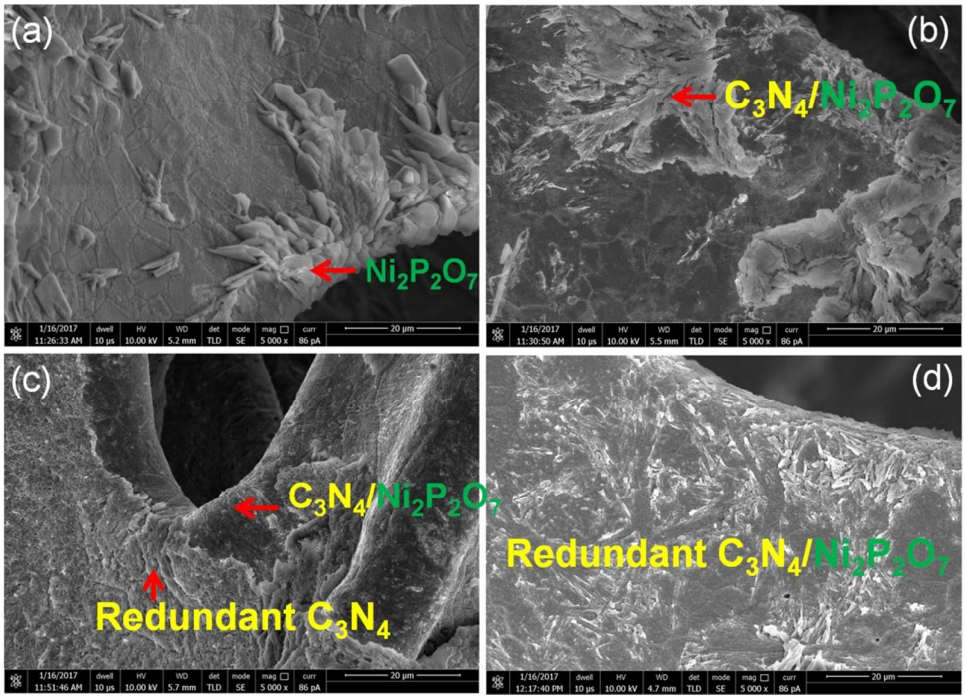

Figure S4 The panoramic SEM images of (a) $Ni_2P_2O_7$, (b) C_3N_4−1/$Ni_2P_2O_7$, (c) C_3N_4−3/$Ni_2P_2O_7$, and (d) C_3N_4−6/$Ni_2P_2O_7$ after charge and discharge approximate 1,000 times at 2 mA cm^{-2}.

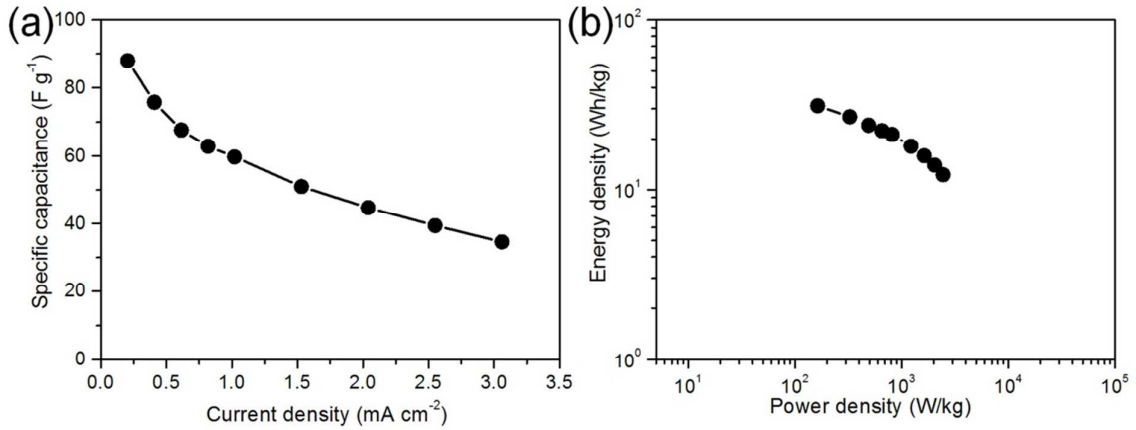

Figure S5 (a) Specific capacitance and (b) Ragone plot of as assembled ASC (The weight of C_3N_4-3/$Ni_2P_2O_7$ is about 2.6 mg, carbon black is about 7.1 mg).

Table S1. A comparison with previously reported transition metal based materials.

No.	Materials	Capacitance	Electrolyte	Ref.
1	Co_3O_4/CC	400 mF/cm^2 at 4 mA/cm^2	3 M KOH	3
2	MnO@C/CC	720 mF/cm^2 at 4 mA//cm^2	3 M KOH	3
3	Li_2Co_2 $(MoO_4)_3$	1.03 F/cm^2 at ~ 1 mA/cm^2	2 M LiOH	4
4	$NiCo_2O_4$ nanoneedle arrays	0.99 F/cm^2 at 5.56 mA/cm^2	2 M KOH	5
5	$Co_{0.33}Ni_{0.67}$DHs/ $NiCo_2O_4$/CFP	~ 2.3 F/cm^2 at 2 mA/cm^2	1 M KOH	6
6	Co_3O_4@MnO_2	0.56 F/cm^2 at 11.25 mA/cm^2	1 M LiOH	7
7	Na-doped $Ni_2P_2O_7$ // AC [a)]	32.6 mF/cm^2 at 0.5 mA/cm^2	PVA/KOH gel	8
8	$Ni_2P_2O_7$ powders // AC [a)]	30 mF/cm^2 at 0.1 mA/cm^2	PVA/KOH gel	9

[a)] as ASCs device

Referneces

(1) Chen, H.; Jiang, J.; Zhang, L.; Xia, D.; Zhao, Y.; Guo, D.; Qi, T.; Wan, H. In Situ Growth of $NiCo_2S_4$ Nanotube Arrays on Ni Foam for Supercapacitors: Maximizing Utilization Efficiency at High Mass Loading to Achieve Ultrahigh Areal Pseudocapacitance. *J. Power Sources* **2014**, *254*, 249–257.

(2) Chen, C.; Zhang, N.; Liu, X.; He, Y.; Wan, H.; Liang, B.; Ma, R.; Pan, A.; Roy, V. A. L. Polypyrrole-Modified $NH_4NiPO_4 \cdot H_2O$ Nanoplate Arrays on Ni Foam for Efficient Electrode in Electrochemical Capacitors. *ACS Sustain. Chem. Eng.* **2016**, *4* (10), 5578–5584.

(3) Yu, N.; Guo, K.; Zhang, W.; Wang, X.; Zhu, M.-Q. Flexible High-Energy Asymmetric Supercapacitors Based on MnO@C Composite Nanosheet Electrodes. *J. Mater. Chem. A* **2017**, *5* (2), 804–813.

(4) Hercule, K. M.; Wei, Q.; Asare, O. K.; Qu, L.; Khan, A. M.; Yan, M.; Du, C.; Chen, W.; Mai, L. Interconnected Nanorods-Nanoflakes $Li_2Co_2(MoO_4)_3$ Framework Structure with Enhanced Electrochemical Properties for Supercapacitors. *Adv. Energy Mater.* **2015**, *5* (10), 1500060.

(5) Zhang, G. Q.; Wu, H. Bin; Hoster, H. E.; Chan-Park, M. B.; Lou, X. W. (David). Single-Crystalline $NiCo_2O_4$ Nanoneedle Arrays Grown on Conductive Substrates as Binder-Free Electrodes for High-Performance Supercapacitors. *Energy Environ. Sci.* **2012**, *5* (11), 9453.

(6) Huang, L.; Chen, D.; Ding, Y.; Feng, S.; Wang, Z. L.; Liu, M. Nickel − Cobalt Hydroxide Nanosheets Coated on $NiCo_2O_4$ Nanowires Grown on Carbon Fiber Paper for High-Performance Pseudocapacitors. *ACS Appl. Mater. Interfaces* **2013**, *5*, 11159–11162.

(7) Liu, J.; Jiang, J.; Cheng, C.; Li, H.; Zhang, J.; Gong, H.; Fan, H. J. Co_3O_4 nanowire@MnO_2 Ultrathin Nanosheet Core/shell Arrays: A New Class of High-Performance Pseudocapacitive Materials. *Adv. Mater.* **2011**, *23* (18), 2076–2081.

(8) Wei, C.; Cheng, C.; Wang, S.; Xu, Y.; Wang, J.; Pang, H. Sodium-Doped Mesoporous $Ni_2P_2O_7$ Hexagonal Tablets for High-Performance Flexible All-Solid-State Hybrid Supercapacitors. *Chem. - An Asian J.* **2015**, *10* (8), 1731–1737.

(9) Pang, H.; Zhang, Y.-Z.; Run, Z.; Lai, W.-Y.; Huang, W. Amorphous Nickel Pyrophosphate Microstructures for High-Performance Flexible Solid-State Electrochemical Energy Storage Devices. *Nano Energy* **2015**, *17*, 339–347.